

Core-Based Intrinsic Fiber-Optic Absorption Sensor for the Detection of Volatile Organic Compounds

GREGORY L. KLUNDER and RICHARD E. RUSSO*

Lawrence Berkeley Laboratory, M/S 90-2024, Berkeley, California 94720 (R.E.R.); and Lawrence Livermore National Laboratory, L-371, Livermore, California 94550 (G.L.K.)

A core-based intrinsic fiber-optic absorption sensor has been developed and tested for the detection of volatile organic compounds. The distal ends of transmitting and receiving fibers are connected by a small cylindrical section of an optically clear silicone rubber. The silicone rubber acts both as a light pipe and as a selective membrane into which the analyte molecules can diffuse. The sensor has been used to detect volatile organics (trichloroethylene, 1,1-dichloroethylene, and benzene) in both aqueous solutions and in the vapor phase or headspace. Absorption spectra obtained in the near-infrared (near-IR) provide qualitative and quantitative information about the analyte. Water, which has strong broad-band absorption in the near-IR, is excluded from the spectra because of the hydrophobic properties of the silicone rubber. The rate-limiting step is shown to be the diffusion through the Nernstian boundary layer surrounding the sensor and not the diffusion through the silicone polymer. The rate of analyte diffusion into the sensor, as measured by the t_{90} values (the time required for the sensor to reach 90% of the equilibrium value), is 30 min for measurements in aqueous solutions and approximately 3 min for measurements made in the headspace. The limit of detection obtained with this sensor is approximately 1.1 ppm for trichloroethylene in an aqueous solution.

Index Headings: Fiber-optic chemical sensors; Volatile organic compounds; Near-IR spectroscopy; Remote sensors.

INTRODUCTION

Recent reports have emphasized the need for environmental monitoring of volatile organic compounds (VOCs).^{1,2} Simple spectroscopic absorption techniques are likely candidates for remote monitoring of organic contaminants in aqueous environments but exhibit several problems. In the ultraviolet and visible, single organic contaminants can be measured quantitatively with little or no qualitative information. Near-infrared (near-IR) spectra can provide quantitative as well as some qualitative information, and IR spectra can yield enough information for a positive identification of the analyte. Although fiber-optic sensors that measure in the IR have been produced,^{3,4} the fibers used to transmit these wavelengths are very fragile and are not practical for use in the field, where they may have to reach depths of several hundred feet. Low-OH quartz fibers offer suitable transmission in the near-IR, are durable, and are commercially available. Absorption spectra in the near-IR can be used for the identification of volatile organic compounds through the C-H, O-H, and N-H overtone vibrations. However, for analysis in the near-IR and IR, the analyte must be separated from the water, which has large absorbance bands throughout this wavelength range. In more

complicated multicomponent systems, chemometrics can be used to interpret spectra obtained in the near-IR. Thus, the near-IR is a very suitable wavelength range for the analysis of organics in aqueous environments.

Wolfbeis⁵ emphasized the importance of separation techniques in conjunction with spectroscopy for fiber-optic chemical sensors (FOCSs). Silicone polymers have been used as membranes for separation of VOCs from water for gas chromatography analysis,⁶⁻⁹ and silicone rubber tubing has been used as a means for purification of VOC-contaminated water.¹⁰ The favorable interaction between nonpolar solvents and silicone polymer could be predicted from their dielectric constants. Zimmerman et al.¹¹ reported enhanced concentrations of trichloroethylene (TCE) in silicone polymers, approximately 250 times that of the concentration in the aqueous solution.

Many commercially available optical fibers use silicone polymers as a cladding material with an additional protective nylon outer jacket. DeGrandpre and Burgess^{12,13} developed a long-path evanescent wave sensor which uses the silicone polymer cladding as a membrane for the detection of the volatile organic compounds. They removed the outer nylon jacket and coiled the optical fiber onto a mechanical support. Detection limits of 1 ppm for TCE in aqueous solution have been reported with a 12-m sensor.¹⁴ A 12-m optical fiber can provide more than 2500 internal reflections and an effective pathlength of 3 to 9 mm, depending on the method of calculation.¹⁵ This pathlength is significantly longer than that achieved by standard attenuated total reflection (ATR) techniques with only a few reflections.

Core-based intrinsic fiber sensors use a section of the fiber core as the sensing region through which all the light passes, not only the evanescent wave. Sigel and co-workers¹⁶⁻¹⁸ developed core-based FOCSs for the detection of ammonia and humidity. Lieberman and co-workers¹⁹ developed a core-based sensor for detecting NO₂ species in the gas phase. Although there are several other examples in the literature, relatively little work has been reported for these sensors. The increased interaction of the light with the analyte should lead to better sensitivity for core-based sensors compared with similar evanescent wave sensors.

In this study, we present data obtained with the use of a core-based sensor with a silicone polymer acting both as a light pipe and as a membrane into which the organic analyte can diffuse. This core-based sensor allows more light to interact with the sample in a smaller, simpler geometry than does the coiled evanescent wave sensor. However, since the silicone polymers are not identical, the two sensors cannot be compared directly. Initial results demonstrating the detection of several volatile or-

Received 19 September 1994; accepted 12 December 1994.

* Author to whom correspondence should be sent.

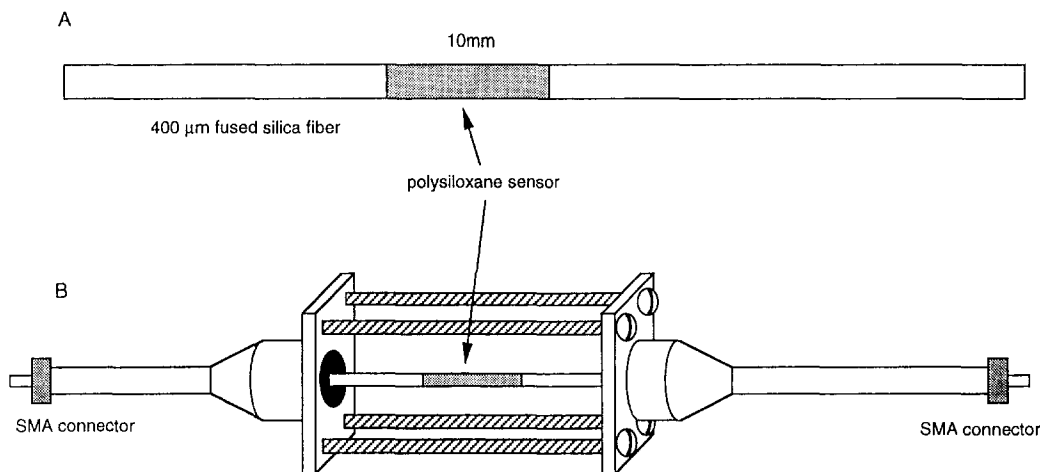


FIG. 1. Diagram of the core-based fiber optic absorption sensor. (A) Fiber sensor dimensions; (B) fiber sensor in its holder connected to SMA connectors.

organics with this sensor as well as results of diffusion kinetics and temperature effects are reported.

EXPERIMENTAL

Fiber-Optic Sensor. The sensor is a solid cylinder of an optically clear silicone rubber that connects two quartz optical fibers (Fig. 1). We used Anhydroguide APC400N low-OH quartz optical fibers (Fiberguide Industries) with a core diameter of 400 μm , a polymer cladding diameter of 500 μm , and a protective nylon jacket diameter of 600 μm . The core refractive index (RI), n_1 , is given as 1.456 and the cladding RI, n_2 , as 1.436 (at 633 nm and 20°C), providing a steady-state numerical aperture (NA) of 0.24 (see Table I). The RI and dn/dT values of the silicone rubber copolymers used for the sensor were not available from the manufacturer. Therefore, we have used constants for polydimethylsiloxane (PDMS) as approximate values. Copolymers consist of two or more polymer components. In this paper, we will use the terms polymer and copolymer interchangeably when referring to the sensor material.

In this study, the silicone polymers used for the sensor material were two different commercially available silicone rubber copolymers: RTV-732 sealant and RTV-3145 (Dow Corning Co., Midland, MI). RTV-732 contains amorphous silica, methyltriacetoxysilane, ethyltriacetoxysilane, and hydroxyterminated dimethylsiloxane. RTV-3145 contains methyl trimethoxysilane, trimethylated silica, polydimethylsiloxane, and dimethyl cyclosiloxanes. The exact chemical composition of the polymers is the proprietary information of the manufacturer. A short (~ 5 mm) length of the protective nylon jacket is removed with hot propylene glycol from the ends of two polished fibers. The sensor is constructed by injecting the silicone rubber copolymer into a 500- μm -i.d. Teflon[®] tube and inserting the polished ends of the optical fibers into both ends of the tube (Fig. 1A). The silicone rubber copolymer is allowed to cure at room temperature for two days. The sensors tested in this work were 1 cm long and 500 μm in diameter. Sensor length is limited by the depth of cure of the polymers. These are one-part polymers which cure at room temperature, when exposed to the moisture in the air, and liberate acetic acid (RTV-732) and methanol

(RTV-3145). Both silicone rubber copolymers adhere strongly to the end of the quartz fiber without any chemical pretreatment. After curing is complete, the sensor is removed from the Teflon[®] tube and fixed in a holder which maintains the sensor in a linear geometry (Fig. 1B). The other ends of the optical fibers are then fitted with standard SMA connectors to allow the sensor to be coupled directly to a spectrometer or to longer optical fiber cables for remote measurements.

Spectrometer. In this study, field conditions were simulated by connecting the sensor to a spectrometer via two 50-m Vis/near-IR fibers (Guided Wave Inc., JC4-50B), which match diameters and numerical apertures of the sensor fiber. A portable single-beam spectrometer (Guided Wave, Model 260) with a tungsten halogen source and lead sulfide detector was used to measure spectra in the near-infrared wavelength range. A 300-lines/mm grating and 1-mm slits were used to obtain spectra from 1100 to 2000 nm, in 1-nm increments. Spectrometer control and data acquisition were achieved with software designed for

TABLE I. Constants and values.

Fiber and sensor parameters	θ_c , critical angle	80.5°
	θ_i , incident angle	85°
	Fiber core diameter	400 μm
	Fiber cladding diameter	500 μm
	NA	0.24
	Sensor diameter	500 μm
	Sensor length	10 mm
Physical constants	Volume thermal expansion (RTV3145)	$7.8 \cdot 10^{-4} \text{ } ^\circ\text{C}^{-1}$
	Volume thermal expansion (RTV-732)	$9.3 \cdot 10^{-4} \text{ } ^\circ\text{C}^{-1}$
	Linear thermal expansion (PDMS)	$2.7 \cdot 10^{-4} \text{ } ^\circ\text{C}^{-1}$
	dn/dT (PDMS)	$-4.2 \cdot 10^{-4}$
	Linear thermal expansion (quartz)	$5.5 \cdot 10^{-7} \text{ } ^\circ\text{C}^{-1}$
	dn/dT (quartz)	$1.28 \cdot 10^{-5}$
Refractive indices	n (quartz)	1.456
	n (PDMS)	1.436
	n (1,1 DCE)	1.425
	n (TCE)	1.475
	n (benzene)	1.498
	n (water)	1.333

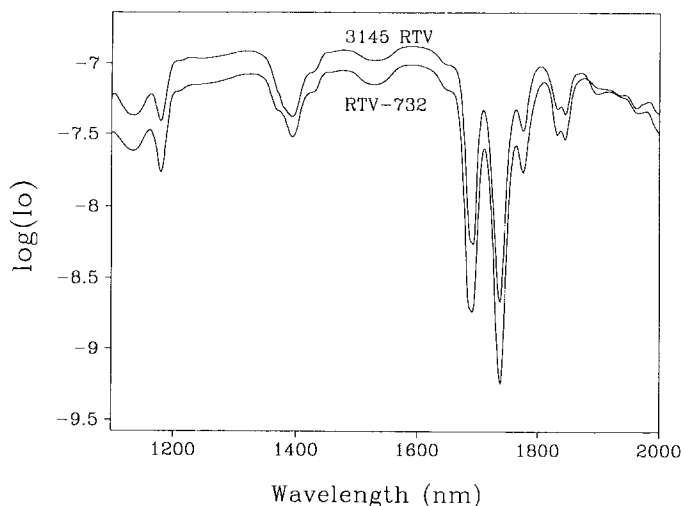


Fig. 2. Optical transmission spectra (reference spectra) for the polymer sensors immersed in water at 18°C. Top obtained with a sensor made from RTV-3145 (Dow Corning) and the bottom from RTV-732 (Dow Corning); both sensors are 500 μm in diameter and 10 mm long.

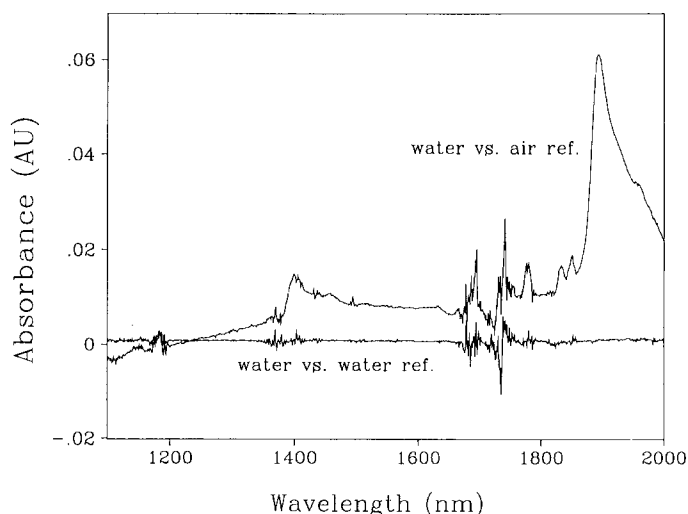


Fig. 3. Background absorbance spectra for the RTV-732 fiber-optic sensor in water at 18°C with reference obtained in (top) air at 21°C, and (bottom) water at 18°C.

the instrument and with a portable computer (Toshiba 3200SXC).

Temperature Control and Sample Preparation. In order to control the temperature of the measurement environment, two thermostated jars (2.75 L each, reference and sample), were connected in parallel to a refrigerated circulator (Neslab Inc., Model RTE-210). Temperatures of aqueous solutions in the two jars were found to be consistent to within 0.2°C. After adjustment of the temperature, solutions were stirred for half an hour to ensure uniform constant temperature before measurements were acquired. Aqueous solutions of the solvents, trichloroethylene and 1,1-dichloroethylene (DCE) (J. T. Baker), were prepared by injecting them into the water-filled sample jar, which has a flat lid and is sealed with an O-ring to minimize losses due to outgassing. Although outgassing losses were minimized, the volatility of the solvents allows us to report only approximate concentrations. Measurements made with a calibrated evanescent wave sensor (discussed previously)¹⁵ provide us with an uncertainty of ± 2 ppm. Unless otherwise stated, reference spectra were obtained in water at the same temperature as the sample. Once the reference spectrum is obtained, the sensor is then transferred to the sample jar and allowed to equilibrate for 0.5 h before sample spectra are acquired.

Benzene vapor was measured by placing a drop (0.05 mL) of benzene in a covered crystal growing dish. This was only a qualitative test of the sensor response, and the concentration in the gas phase was unknown. Headspace measurements of TCE were made in the thermostated jars filled to half of the total volume (1.38 L) with a 20-ppm TCE solution. The sensor was inserted, the jar was sealed, and the solution was stirred at a constant rate.

RESULTS AND DISCUSSION

Sensor Response. For acquisition of absorption spectra with a single-beam spectrometer, a reference transmission spectrum (I_0) is measured in water at a constant temperature and is stored in the computer. An absorption spectrum is obtained by measuring a transmission spectrum

(I) of the sample and calculating $A = -\log(I/I_0)$. An absorption spectrum without analyte obtained under the same conditions as the reference will show the background noise associated with the system. Changing a parameter from the reference conditions provides an absorption spectrum which shows the response of the system due to that parameter, provided that it is independent of all the other parameters. In Fig. 2, the optical transmission spectra (reference) for two fiber sensors in water at 18°C are plotted as the logarithm of the power [$\log(I_0)$] vs. wavelength. Because the refractive index of the polymer (1.436) is greater than that of the surrounding water (1.333), total internal reflection is maintained through the sensor. The emission from the quartz-halogen lamp, transmission of the optical fiber, and detector response are unstructured over this wavelength range. The characteristic bands are overtone absorption bands of the C-H bonds in the silicone polymers. The first overtones of CH_3 and CH_2 vibrations are the strongest bands at 1692 and 1738 nm, with weaker combination bands appearing at 1395 nm and the second overtones around 1178 nm. The RTV-3145 sensor has slightly better light transmission but is generally indistinguishable from the absorption profile of RTV-732 because of the large number of CH_2 and CH_3 bonds.

Background absorption spectra for the RTV-732 sensor are presented in Fig. 3. The top spectrum was obtained in water at 18°C with the reference obtained in air at an ambient temperature of 21°C. The large peak at 1892 nm, as well as a smaller peak at 1397 nm, is due to water absorption. Although silicone polymers are known to be hydrophobic, a finite amount of water sorbs into the material. Watson et al. reported a saturation concentration of 40 mol/m³ water in polydimethylsiloxane (PDMS).²⁰ The sloping baseline and other structure are due to the differences in temperature from the reference, and resultant changes in the RI of the polymer. These effects will be discussed in more detail in the next section. When the reference and background spectra are obtained under the same conditions, the background is flat and has lower noise, as seen in the bottom spectrum, where both ref-

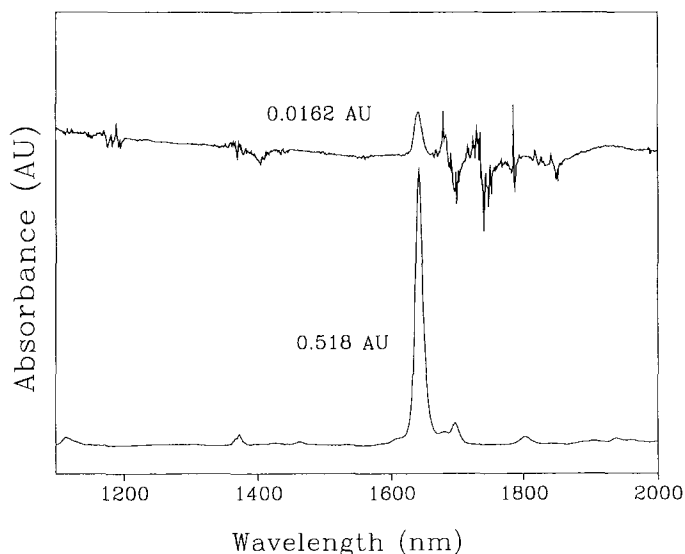


FIG. 4. Absorbance spectra for 20-ppm TCE with the RTV-732 polymer sensor (top) and 1-mm cuvette spectrum of pure TCE (bottom) with the use of the same spectrometer.

erence and background were obtained in water at 18°C. Fluctuations of the background absorbance signal are still present in the region from 1700 to 1800 nm and, to a lesser extent, around 1400 nm. These deviations are the result of the lower light transmission (I_0) due to absorption by the silicone copolymer sensor (see Fig. 2), where smaller changes in the transmitted intensity (I) will produce larger changes in the absorbance. In the wavelength ranges where the reference transmission is not severely attenuated because of absorption of the silicone rubber copolymer, the peak-to-peak noise is measured to be about 0.3 mAU.

Spectra showing the RTV-732 sensor response to TCE, DCE, and benzene are presented in Figs. 4–6, respectively. Each figure also shows the absorbance spectra of the pure solvent in a standard 1-mm-path quartz cuvette with the use of the same spectrometer. Similar spectra (not shown) were obtained with the sensor made with the RTV-3145 copolymer. The primary absorption peak for TCE appears at 1642 nm, which is outside the wavelength range of the background fluctuations. When exposed to TCE, the background fluctuations in the 1680–1800 nm range appear different from those observed in Fig. 3. This difference is due to a change in the RI of the silicone rubber copolymer matrix (copolymer and analyte) from the initial RI at which the reference spectrum was acquired. This pattern includes changes due to the different RI of the solvent and any swelling that may induce changes in the RI of the copolymer. The absorbance spectrum for a 20-ppm aqueous solution of DCE also shows RI effects which are more extreme than those observed with TCE. Two reasons for this observation are a larger partition coefficient for DCE into PDMS and the low RI of DCE (1.425). Ache and co-workers showed that the partition coefficient is a function of both the boiling point and the solubility of the analyte.^{11,21} Thus, DCE, which has a lower boiling point than TCE, would be expected to have a larger partition coefficient. In addition to the background fluctuations, the significant slope in the baseline is also due to the RI changes of the polymer, which will be dis-

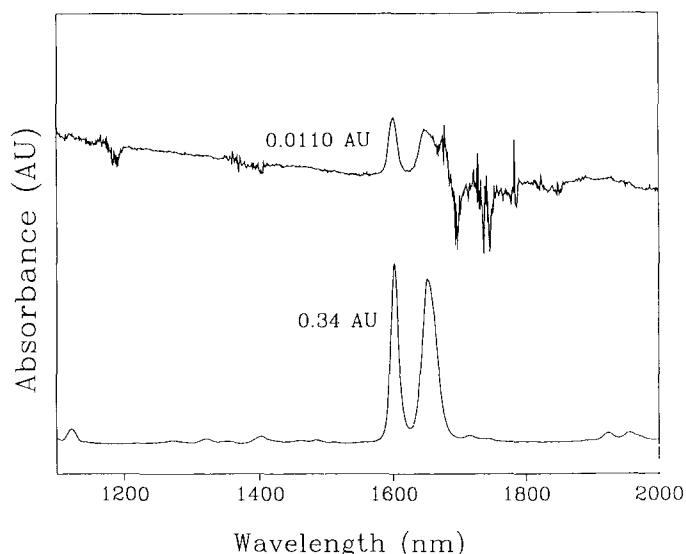


FIG. 5. Absorbance spectra for 20-ppm 1,1-DCE with the RTV-732 polymer sensor (top) and 1-mm cuvette spectrum of pure 1,1 DCE (bottom) with the use of the same spectrometer.

cussed further in the next section. Figure 6 shows the response of the sensor to a drop (~0.05 mL) of benzene placed in a covered crystal growing dish with the reference obtained in air at the same temperature. This was a qualitative experiment, and the concentrations of benzene in the air and sensor were unknown.

Although a calibration curve has not been generated, an estimate of the limit of detection can be calculated. The background noise is 0.3 mAU, and a 20-ppm TCE solution provided a response of 0.0162 AU. For a signal-to-noise ratio of 3:1, the detection limit for TCE can be estimated at approximately 1.1 ppm. It should be noted that the sensor is completely reversible. All the spectra which appear in this report were acquired with the same sensor. Once removed from the solution, the volatile compounds rapidly escape from the sensor, and a baseline

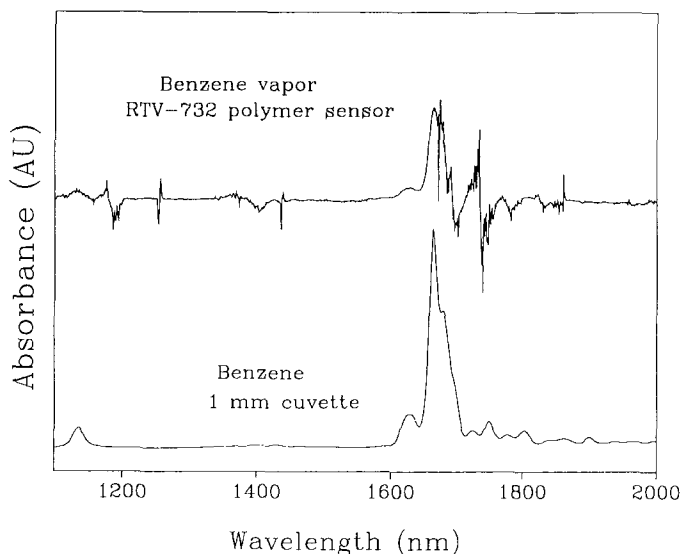


FIG. 6. Benzene vapors into the polymer RTV-732 (top) compared to 1-mm cuvette spectrum of pure benzene with the use of the same spectrometer.

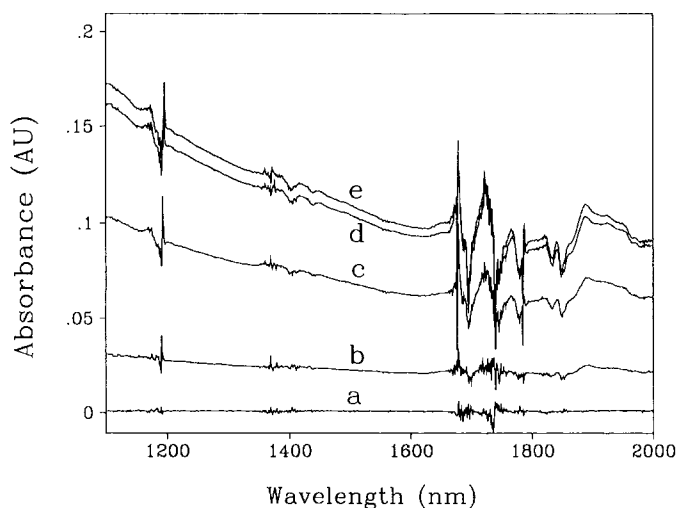


FIG. 7. Temperature dependence of the polymer sensor. Reference in water at 11°C and spectra measured in water (a) 11°C, (b) 14°C, (c) 17°C, (d) 20°C, (e) 23°C.

response is obtained in several minutes. While the sensor lifetime is unknown, we have used the same sensor for a year with no significant loss in performance.

Temperature Effects. As described for the data in Fig. 3, small changes in temperature from the reference affect the response of the sensor. Differences in temperature of the analyte solution from the reference can have several effects on the polymer, including swelling and RI changes. With a reference spectrum obtained at 11°C, the data in Fig. 7 (a–e) show the effect of temperature on the background spectra (no analyte) at 11, 14, 17, 20, and 23°C, respectively, for the RTV-732 sensor. According to the equation of thermal expansion, swelling due to temperature changes should follow a linear trend:

$$r = r_0(1 + \alpha T) \quad (1)$$

where r is the radius at temperature, T ; and r_0 is the radius at 0°C.²² The manufacturer reports volumetric thermal expansion coefficients for RTV-3145 and RTV-732 as 7.8×10^{-4} and 9.3×10^{-4} (°C⁻¹), respectively. Volume thermal expansion coefficients are typically three times the linear thermal expansion coefficients.²² The coefficient of linear thermal expansion, α , for polydimethylsiloxane (PDMS) is listed as 2.7×10^{-4} (°C⁻¹),²³ and the value for quartz is 5.5×10^{-7} (°C⁻¹),²⁴ which is relatively small and can be neglected. Light losses due to a 3°C temperature change would be small [0.16% (0.7 mAU)], strictly on the basis of increasing the diameter of the silicone sensor with respect to the quartz fiber core. Losses due to swelling are independent of wavelength and contribute to the observed baseline offset of the spectra. Since the observed offset for a 3°C temperature change is greater than the 0.7 mAU predicted, other factors need to be considered. Swelling of the polymer may also lead to increases in the pore sizes and increase losses due to scattering, although this effect has not been confirmed. The data in Fig. 7 also show that there are wavelength-dependent losses, as observed by the sloping baseline. The wavelength-dependent losses are due to changes in the RI and the reflectivity at the two polymer/quartz interfaces. According to Har- rick,²⁵ the reflectivity change can be approximated as $\Delta(n_2/$

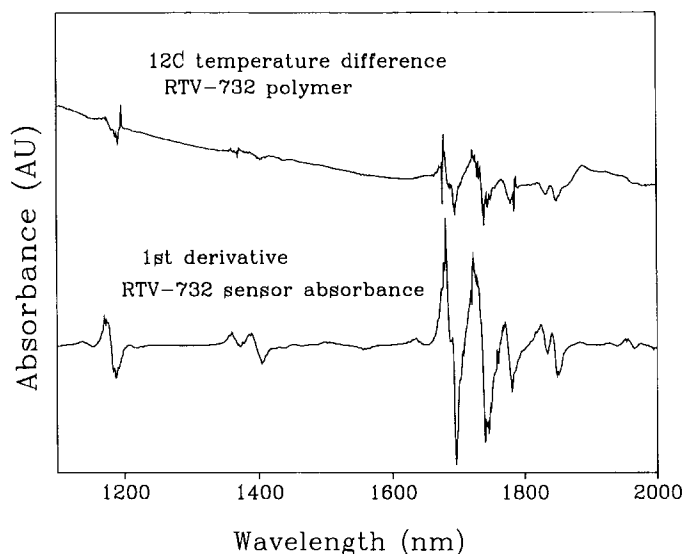


FIG. 8. Background absorbance with a 12°C temperature difference from the reference (Fig. 7e) compared to the first derivative of the absorbance (Δ AU) of the RTV-732 sensor.

n_1), where n_2 is the RI of the incident reflecting surface and n_1 is the RI of the originating material. The RI of the fused-silica fiber core decreases with increasing wavelength and has a dn/dT value of $+1.28 \times 10^{-5}$ (°C⁻¹).²⁴ The dn/dT for polydimethylsiloxane (PDMS) is -4.2×10^{-4} . The first surface to consider is the fiber/sensor interface, where n_1 is the RI of the fiber core and n_2 is the RI of the copolymer sensor. In this case, increasing the temperature will decrease reflectivity losses in comparison to the reference spectrum. The second surface is the sensor/fiber interface, where n_1 is the RI of the copolymer sensor and n_2 is the RI of the fiber core, and it will cause an increase in reflectivity with increases in temperature. Decreasing the temperature from the reference will have the same net effect.

In the wavelength range of the polysiloxane absorption peaks, the structure due to temperature changes from the reference follows the first derivative of the absorbance in the absence of any analyte, as seen in Fig. 8. We observed this relationship previously¹⁵ with an evanescent wave sensor where the refractive index followed a first derivative-like profile. A water absorption peak appears to be growing in at 1892 nm with increasing temperature. This observation is due to the length of time that the sensor resided in the water, allowing more water to sorb into the polymer. These measurements were made consecutively, and thus the sensor remained immersed in the water bath for several hours.

As discussed with respect to Fig. 5, the presence of DCE also results in a sloping baseline similar to that observed by increasing the temperature. This result is also due to lowering the RI of the sensor, since the analyte/polymer has a lower RI than that of the polymer sensor. Swelling of the polymer also occurs in the presence of analyte, which reduces the effective RI. It is expected that TCE and benzene, which have higher RIs than PDMS does, would have the opposite effect and would result in a positive sloping background similar to that observed in Fig. 3. Since this was not observed, the actual RI of sensor

material may be higher than that of PDMS and much closer to the values of TCE and benzene.

Diffusion and Kinetics. Conzen et al.²¹ discussed the effects of diffusion of volatile organic compounds into polysiloxane cladding material for an evanescent wave fiber-optic sensor. Their data indicated that the rate-limiting step is the diffusion of the organic analyte through the Nernstian boundary layer and not the diffusion through the bulk polymer. Because of the lengths and angles of Si-C bonds, polysiloxane polymers are very flexible and exhibit a freedom of motion with fluid-like qualities. Diffusion coefficients for organic solvents in silicone rubbers are on the order of $10^{-6} \text{ cm}^2 \text{ s}^{-1}$ ^{20,26} and in aqueous solution on the order of $10^{-5} \text{ cm}^2 \text{ s}^{-1}$.²¹

According to Fick's second law, the time-dependent concentration is given by

$$dc/dt = D(d^2c/dx^2) \quad (2)$$

where c is the concentration, t is time, D is the diffusion coefficient, and x is the pathlength of the diffusing substance. In cylindrical coordinates assuming only radial diffusion, this expression becomes

$$dc/dt = (D/r) * d(r dc/dr)dr \quad a < r < b \quad (3)$$

where a and b are the inner and outer radii of the cylinder, respectively. In the case of a solid cylinder, the inner diameter, a , is zero. For low concentrations the diffusion can be considered constant, and the concentration at a given time, t , can be approximated by

$$c(t) = c_e(1 - \exp(-kt)) \quad (4)$$

where k is a constant that takes into account the diffusion coefficient and geometry of the sensor, and c_e is the concentration of analyte in the sensor at equilibrium. Assuming a direct linear correlation between concentration and absorption:

$$c(t) \propto A(t) \quad (5)$$

we can use the absorbance data to represent the concentration in Eq. 4. The data in Fig. 9 show background-corrected absorbance measurements vs. time, for TCE in solution. The lines through the data represent a solution to Eq. 4. The excellent fit of the data to the theoretical predictions confirms the work of Conzen et al.,²¹ showing the Nernstian boundary layer to be the rate-limiting step. Response times are typically reported by t_{90} values, the time it takes for the sensor to reach 90% of its equilibrium response. The t_{90} values are 1800 s for the RTV-732 sensor and 2000 s for the RTV-3145 sensor. It appears that the RTV-732 sensor has a higher partition coefficient for TCE. However, a quantitative comparison of the two sensors should not be made on the basis of these data because of the volatility of the analyte and any changes in the concentration that may have occurred. The open squares are the data obtained with the RTV-732 sensor made in the headspace above a nominal 20-ppm TCE solution. The t_{90} value is 200 s, which is consistent with the diffusion through the aqueous Nernstian boundary as the rate-limiting step. Increased diffusion kinetics due to the lack of an aqueous layer have also been reported by Pawliszyn and co-workers.²⁷

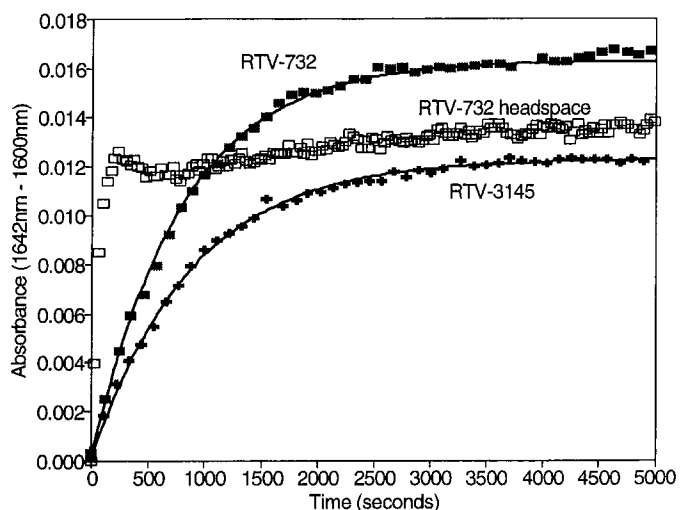


FIG. 9. Absorption vs. time showing the diffusion of TCE (20 ppm) into the RTV-732 and RTV-3145 sensors measured in an aqueous solution and in the headspace (RTV-732 only).

CONCLUSION

A core-based fiber-optic sensor has been described which is suitable for remote, *in situ* measurements. It is based on a reversible physical interaction rather than a chemical reaction. Analysis can be made directly in water and may allow for depth profiling, which is important since many organic ground-water contaminants are denser than water. The small size and ruggedness are ideal for field applications, and the simplicity of the design should be suitable for commercial manufacturing.

The detection limit for TCE in an aqueous solution is approximately 1.1 ppm, which is on par with the detection limits of the evanescent field absorption sensor reported by Bürck et al.¹⁴ Sensor length has been limited to approximately 1 cm with the one-part room-temperature vulcanized silicone polymers used in this study. We have experimented with different types of silicone polymers (e.g., catalyzed two-part systems), which can provide longer sensors and are more optically clear. However, lack of strong adhesion of the polymer to the small area of the quartz fiber tip has limited our studies with these sensors. Silicone polymers can be easily modified, providing changes in the optical clarity, rigidity, porosity, hydrophobicity, and partition coefficients. Thus, there is a large window of opportunity for tailoring silicone polymer sensors for the analytes of interest.

1. R. Rajagopal and P. C. Li, *Am. Environ. Lab.* **4**, 16 (1994).
2. J. N. Driscoll, *Environ. Test. Anal.* **January/February**, 23 (1993).
3. R. Krška, K. Taga, and R. Kellner, *Appl. Spectrosc.* **47**, 1484 (1993).
4. J. Heo, M. Rodrigues, S. J. Saggese, and G. H. Sigel, Jr., *Appl. Opt.* **30**, 3944 (1991).
5. O. S. Wolfbeis, *Fiber Optic Chemical Sensors and Biosensors* (CRC Press, Boca Raton, Florida, 1991).
6. Z. Zhang and J. Pawliszyn, *Anal. Chem.* **65**, 1843 (1993).
7. K. F. Pratt and J. Pawliszyn, *Anal. Chem.* **64**, 2101 (1992).
8. K. F. Pratt and J. Pawliszyn, *Anal. Chem.* **64**, 2107 (1992).
9. C. L. Arthur and J. Pawliszyn, *Anal. Chem.* **62**, 2145 (1990).
10. A. R. J. Andrews, A. Zlatkis, M. T. Tang, W. Zhang, and H. Shanfield, *Environ. Sci. Technol.* **27**, 1139 (1993).
11. B. Zimmerman, J. Bürck, and H.-J. Ache, *KfK Report No. 4967* (Kernforschungszentrum, Karlsruhe, 1991).
12. M. D. DeGrandpre and L. W. Burgess, *Anal. Chem.* **60**, 2582 (1988).

13. M. D. DeGrandpre and L. W. Burgess, *Appl. Spectrosc.* **44**, 273 (1990).
14. J. Bürck, J.-P. Conzen, and H.-J. Ache, *Fres. J. Anal. Chem.* **342**, 394 (1992).
15. G. L. Klunder, J. Bürck, H.-J. Ache, R. J. Silva, and R. E. Russo, *Appl. Spectrosc.* **48**, 387 (1994).
16. Q. Zhou, D. Kritz, L. Bonnell, and G. H. Sigel, Jr., *Appl. Opt.* **28**, 2022 (1989).
17. Q. Zhou, M. R. Shahriari, D. Kritz, and G. H. Sigel, Jr., *Anal. Chem.* **60**, 2317 (1988).
18. M. R. Shahriari, Q. Zhou, and G. H. Sigel, Jr., *Opt. Lett.* **13**, 407 (1988).
19. E. M. Schmidlin, E. A. Mendoza, D. J. Ferrell, S. J. Syracuse, A. N. Khalil, and R. A. Lieberman, *SPIE Proc.* **2068**, 41 (1993).
20. J. M. Watson, G. S. Zhang, and P. A. Payne, *J. Membrane Sci.* **73**, 55 (1992).
21. J.-P. Conzen, J. Bürck, and H.-J. Ache, *Appl. Spectrosc.* **47**, 753 (1993).
22. *CRC Handbook of Chemistry and Physics*, R. C. Weast, Ed. (CRC Press, Boca Raton, Florida, 1978–1979), 59th ed., p. F-122.
23. GE Silicones product information for GE RTV615 silicone rubber, Publication No. CDS4415 (GE Silicones Inc., Waterford, New York, 1991).
24. *Melles Griot Optics Guide 5* (Melles Griot, Irvine, California, 1990), pp. 3–5.
25. N. J. Harrick, *Internal Reflection Spectroscopy* (Interscience, New York, 1967).
26. C. J. Guo, D. DeKee, and B. Harrison, *Chem. Eng. Sci.* **47**, 1525 (1992).
27. D. Louch, S. Motlagh, and J. Pawliszyn, *Anal. Chem.* **64**, 1187 (1992).